# Representational Similarity Reveals Sleep-Dependent Memory Consolidation Impaired by Simulated OSA

**Ting Pan[1], Xiaozhuo Bai[1], Yang Luo[1], Yunkai Shi[1] & Yin Tian (tianyin@cqupt.edu.cn) [1, 2,*]**

[1]School of Life Health Information Science and Engineering, Chongqing University of Posts and Telecommunications

[2]School of Computer Science and Technology, Chongqing University of Posts and Telecommunications

## Abstract

Obstructive sleep apnea (OSA) is strongly linked to memory consolidation deficits, yet the neural mechanisms by which OSA disrupts memory consolidation remain poorly understood. Clarifying these mechanisms is crucial for identifying early biomarkers and developing targeted interventions to mitigate OSA-related cognitive decline. This study used a within-subject pre-sleep versus post-sleep design in healthy volunteers, comparing normal sleep with simulated OSA (via overnight airflow restriction) while measuring behavioral performance and EEG during visuospatial and verbal memory consolidation tasks. Results revealed that normal sleep produced significant post-sleep behavioral gains, enhanced representational similarity (RSA), strengthened long-range functional connectivity, and increased theta-gamma phase-amplitude coupling (PAC) with optimized phase preference. Simulated OSA abolished these improvements or even caused deterioration, accompanied by reduced RSA, weakened connectivity, and diffuse PAC patterns. These multi-level findings provide mechanistic insights for future analyses of OSA-related cognitive impairments.

**Keywords:** OSA; memory consolidation; RSA; functional connectivity; PAC

## Instruction

Obstructive Sleep Apnea (OSA) is a prevalent sleep breathing disorder characterized by intermittent hypoxia and sleep fragmentation, impacting hundreds of millions of adults globally (Lastra et al., 2025). Untreated OSA is associated with severe cognitive impairment, particularly deficits in memory, which may progress to mild cognitive impairment (MCI) or even dementia (Zhang et al., 2025). Memory consolidation refers to the neural processing process that converts short-term memory into stable and long-lasting long-term memory, which is completed depending on sleep stages (Kim et al., 2025). In recent years, neuroimaging studies have shown that the memory consolidation process is impaired in patients with OSA, accompanied by abnormal changes in functional connectivity of memory-related brain regions. (Wu et al., 2025).

Representational Similarity Analysis (RSA) is a multivariate approach that quantifies the geometric structure of brain representations by computing similarity matrices between neural activation patterns across different stimuli or conditions (Kriegeskorte et al., 2008). Compared to traditional univariate activation analyses, RSA allows comparison of representational consistency across modalities or between individuals and has been widely applied in research on vision, memory, decision-making, and other domains. Sleep disruption caused by OSA may impair the stability of neural representations, thereby providing a potential explanation for memory consolidation deficits in patients (Suh et al., 2021).Furthermore, brain network analysis constructs functional connectivity networks using methods such as the Weighted Phase Lag Index (WPLI) and imaginary coherence (iCOH) to reveal synchronization between brain regions (Liu et al., 2025); Phase-Amplitude Coupling (PAC) quantifies the strength of cross-frequency coupling, such as the role of theta-gamma coupling in memory encoding (Zhang et al., 2024). These methods can capture dynamic network reorganization and abnormal oscillatory coupling in the context of OSA, offering mechanistic explanations for cognitive impairment.

However, the specific neural mechanisms by which OSA disrupts sleep-dependent consolidation of memory consolidation remain unclear. Existing studies are primarily limited by the lack of controlled within-subject designs, which prevents the isolation of the acute effects of sleep disturbance on multi-level cognitive processes, from behavioral performance to RSA, long-range functional connectivity, and cross-frequency oscillatory coupling. Although sleep is known to actively link short-term memory maintenance with long-term declarative memory systems through hippocampal-neocortical dialogue, how OSA specifically impairs this interaction is still poorly understood.

To address these research gaps, the present study makes the following contributions:

1.The experimental design employed in this study enables relatively pure and controlled manipulation of sleep disturbance, while allowing paired pre-sleep and post-sleep comparisons within the same participants. This approach more clearly isolates the causal impact of acute sleep disruption on memory consolidation;

2.This study employs multi-level analyses to collectively reveal how genuine sleep promotes the consolidation of visuospatial and verbal memory, as well as how simulated OSA disrupts these sleep-related cognitive advantages;

3.This approach not only provides clearer causal evidence for the mechanistic role of sleep in memory consolidation, but also holds potential clinical value for the early identification, risk stratification, and targeted intervention of OSA-related cognitive impairment.



In G. Boleda, I. Dautriche, M. Maldonado, C. Saldana and T. Torrent (Eds.), *Proceedings of the 48th Annual Conference of the Cognitive Science Society* 

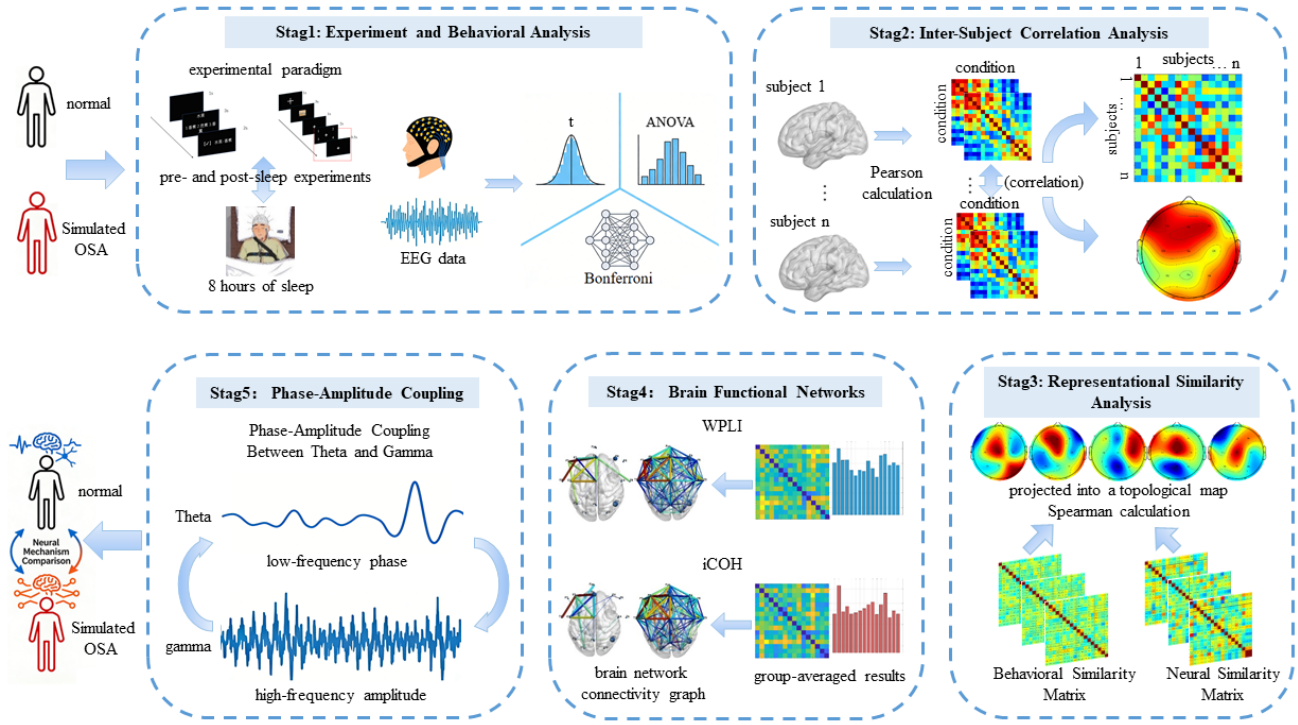


Figure 1: Analytical Framework.

## Method

### Behavioral Data Statistical Analysis

Statistical analyses were performed on the behavioral indicators of the memory task. First, the mean accuracy and reaction time(RT) of each participant were calculated under the pre-sleep and post-sleep conditions. For both the normal group and the simulated OSA group, independent-samples t-tests were conducted on each task indicator for an overall comparison between pre-sleep and post-sleep conditions.

A one-way Analysis of Variance (ANOVA) was also conducted, with group as the independent variable (Hou et al., 2022).

$$F = \frac{MS_{between}}{MS_{within}} = \frac{SS_{between}/df_{between}}{SS_{within}/df_{within}} \quad (1)$$

Where $SS_{between}$ represents the sum of squares between groups, and $SS_{within}$ denotes the sum of squares within groups.

### Inter-Subject Correlation (ISC) and RSA

Pearson's correlation coefficient was adopted to examine the similarity of functional connectivity patterns across participants in specific brain regions (or electrodes) (Nastase et al., 2019). Inter-subject correlation for behavioral data (ISC-behavior) (Chen et al., 2020) was computed based on the RT sequences of each participant pair, while inter-subject correlation for EEG data (ISC-EEG) was calculated based on the EEG time courses of each participant pair at the same electrodes and time points (Kandeepan et al., 2023).

$$r_{XY} = \frac{\sum_{i=1}^{n}(X_i - X)(Y_i - Y)}{\sqrt{\sum_{i=1}^{n}(X_i - \overline{X})^2}\sqrt{\sum_{i=1}^{n}(Y_i - \overline{Y})^2}} \quad (2)$$

where $X_i, Y_i$ denotes the i-th observation of $X, Y$, and $\overline{X}, \overline{Y}$ denotes the sample mean of variable $X, Y$, i.e., the average of all observations of $X, Y$.

First, for each frequency band (theta, alpha, beta, gamma, and the full frequency band), inter-subject neural similarity matrices were calculated under pre-sleep and post-sleep conditions, respectively. Pairwise Pearson correlation coefficients of EEG patterns during task performance were used to reflect the similarity of neural responses between individuals. In the visuospatial memory experiment, behavioral similarity matrices were constructed separately for two main behavioral indicators: RT for old-new picture discrimination and RT for quadrant localization judgment. For each indicator, pairwise Pearson correlation coefficients between subjects were calculated, resulting in two independent behavioral similarity matrices for each of the two groups (normal group and OSA simulation group) across the two time points (pre-sleep and post-sleep). In the verbal memory experiment, the matrices were constructed based on two indicators: RT and accuracy rate. To quantify the RSA, we extracted the upper triangular elements of each similarity matrix and performed calculations using the Spearman's rank correlation coefficient (Huang et al., 2025). This non-parametric method can effectively address the ordinal nature of similarity rankings and reduce the impact of outliers. Differential topological maps were used to visually demonstrate the inter-group differences in the similarity and

distribution patterns of functional connectivity.

$$r_s = \frac{\sum_{i=1}^{n} R(X_i)R(Y_i) - nR(X)R(Y)}{\sqrt{\left[\sum_{i=1}^{n} R(X_i)^2 - n\overline{R}(X)^2\right]\left[\sum_{i=1}^{n} R(Y_i)^2 - n\overline{R}(Y)^2\right]}} \quad (3)$$

Where, $R(X_i)$ denotes the rank of variable $X_i$, and $\overline{R}(X)$ represents the mean rank of variable X.

## Construction of Brain Functional Networks and PAC Analysis

For brain network construction, two widely recognized and commonly used methods, WPLI and iCOH, were selected and employed to build undirected functional connectivity networks across the theta (4–8 Hz), alpha (8–13 Hz), beta (13–30 Hz), and gamma (30–45 Hz) frequency bands. Both methods can effectively mitigate the common disruptive effects of volume conduction and common source artifacts (Vinck et al., 2011).

The formula for WPLI is as follows:

$$\text{WPLI} = \frac{\left|\sum_{t-1}^{N} W(t) \cdot sgn\left(\sin\left(\Delta\phi(t)\right)\right)\right|}{\sum_{t-1}^{N} W(t)} \quad (4)$$

Where, $W(t)$ denotes the weight function, and $\phi(t)$ represents the phase difference.

The formula for iCOH is as follows:

$$iCOH_{xy}(f) = imag\left(C_{xy}(f)\right) \quad (5)$$

Where, $C_{xy}(f)$denotes the coherence spectrum.

We performed averaging on the connectivity matrices and node degrees, respectively, to obtain the group-averaged WPLI/iCOH matrices and mean node degrees. For comparisons between pre-sleep and post-sleep states as well as inter-group differences, we adopted the network-based statistics (NBS) method for multiple comparison correction, with a total of 10,000 permutations conducted (Zalesky et al., 2010).

To further explore the changes in cross-frequency oscillatory coupling during memory consolidation processing, this study simultaneously calculated the modulation strength of the phase of the theta band on the amplitude of the gamma band (Daume et al., 2024). In the calculation of PAC, the mean vector length method was adopted to quantify the coupling strength (Hülsemann et al., 2019), The formula is as follows:

$$\vec{z} = A_{HF}(t) \cdot e^{i\phi LF(t)} \quad (6)$$

where, $i\phi LF(t)$ represents the phase of the low-frequency signal, and $A_{HF}$ represents the envelope of the high-frequency signal.

For each phase bin, the mean value of the gamma oscillation amplitude at the corresponding time points is calculated. The amplitude value of each bin is regarded as the length of a complex vector, and its direction is determined by the central phase angle of the bin. The average result of these vectors is then computed, and the modulus of this average result is defined as the Modulation Index (MI) (Canolty et al., 2006). This index reflects the degree to which the gamma amplitude distribution deviates from a uniform distribution, with a value range of [0, 1] (Tort et al., 2010).

$$\text{MI} = \left|\frac{1}{N}\sum_{t-1}^{N} \vec{z}(t)\right| \quad (7)$$

The PAC vectors of all valid participants were aggregated to calculate the cross-subject averaged modulation index curve. The phase axis was extended to the range of $0^\circ$ to $360^\circ$ in visualization, corresponding to 36 data points. The formula for cross-temporal and cross-subject averaging is given as follows:

$$\overline{MI}(\phi_i) = \frac{1}{N_f \cdot N_t}\sum_{f=1}^{N_f}\sum_{t=1}^{N_t} MI(\phi_i, f, t) \quad (8)$$

wherein, $\phi_i$ denotes the i-th phase bin.

To examine the overall pre-sleep to post-sleep changes and intergroup differences between the normal group and the simulated OSA group, a repeated-measures ANOVA was performed on the population-averaged modulation index vectors, and paired or independent-samples t-tests were conducted on the maximum MI values and the peak phase positions. Bonferroni correction was applied for multiple comparisons, with the significance level set at $p < 0.05$.

# Experiment

## Data Description

A total of 18 healthy adult volunteers were recruited in this study. The participants were divided into two groups: the normal group (with normal sleep following the first experiment) and the simulated OSA group (who wore a mask to restrict airflow at night after the first experiment, which was verified by polysomnography to induce moderate intermittent hypoxia and arousals.). To control for individual differences, the simulated OSA group consisted of the same batch of volunteers who had participated in the first experiment under normal sleep conditions as far as possible.

## Experimental Paradigm

This study adopted the visuospatial memory task and the verbal memory task, and each task consisted of three phases: encoding, maintenance and recognition. All participants completed the pre-sleep memory task at 22:00 on the experimental day, with simultaneous EEG data collection (Chen et al., 2025). The participants then entered the sleep phase: the normal group had an 8-hour normal sleep session, while the simulated OSA group received sleep intervention with a mask worn. All participants were awakened at 7:00 the next morning and, upon awakening, completed the identical memory task again, with simultaneous collection of EEG and behavioral data for the task a second time.

## Data Preprocessing

Raw EEG recordings in the EDF format typically contain substantial noise and artifacts, and an automated batch processing pipeline was implemented using the EEGLAB toolbox for this preprocessing procedure. The main steps included: reading EDF files, performing band-pass filtering,

automatically detecting bad channels based on kurtosis and repairing them via spherical interpolation, applying average reference, conducting Independent Component Analysis (ICA) decomposition, and combining ICLabel for automatic component classification to remove ocular and muscular artifact components with a confidence level of ⩾90%. The entire pipeline was completed in a single run on the full behavioral EEG dataset, ultimately outputting cleaned EEG signals.

## Results and Analysis

### Behavioral Data Statistical Analysis

For visuospatial memory, the RT of the normal group exhibited a post-sleep decreasing trend in both tasks. Specifically, in the old-new picture discrimination task, RT decreased significantly from 1.398±0.232 s at pre-sleep to 1.264 ± 0.287 s at post-sleep (F=9.03, p=0.013). In the quadrant judgment task, the change in RT was non-significant, with values shifting from 0.765±0.223 s to 0.789 ±0.117 s (F=0.22, p=0.650). In contrast, the simulated OSA group showed only a slight decrease or marginal prolongation in RT. In the old-new picture discrimination task, RT changed from 1.177±0.198 s at pre-sleep to 1.184±0.219 s at post-sleep (F=0.069, p=0.796); in the quadrant judgment task, RT altered from 0.666±0.231 s to 0.649±0.179 s (F=0.091, p=0.753). No statistically significant differences were detected for the simulated OSA group in either task.

For verbal memory performance, the accuracy rate of the normal group increased significantly from 0.748±0.085 at pre-sleep to 0.825±0.076 at post-sleep (F=15.41, p=0.002), and RT was also shortened significantly from 1.807±0.207 s at pre-sleep to 1.735 ± 0.188 s at post-sleep (F=7.94, p=0.023). In comparison, the simulated OSA group only demonstrated a slight, non-significant increase in accuracy rate, with values rising from 0.786±0.106 at pre-sleep to 0.863±0.759 at post-sleep (F=4.28, p=0.058); additionally, their RT was prolonged significantly, shifting from 1.728± 0.243 s at pre-sleep to 1.813±0.264 s at post-sleep (F=7.57, p=0.027).

### Results of ISC and RSA

In both types of tasks, the normal group exhibited a consistent pattern of a significant increase in ISC following sleep, with an expansion of warm-color regions and a reduction in inter-individual differences, indicating a marked convergence of neural representations across individuals (Simony et al., 2016). In contrast, the simulated OSA group showed a pronounced pattern of inter-individual representational divergence/heterogeneity (dominated by cool-color regions), with significantly dispersed inter-individual neural representations, as well as fragmented and increasingly heterogeneous memory patterns (Djonlagic et al., 2021; Wallace et al., 2013). This cross-task consistent intergroup difference in neural patterns demonstrates the consolidating effect of normal sleep on memory and the extensive impairment of the neural mechanisms underlying memory induced by sleep apnea-like disturbances.

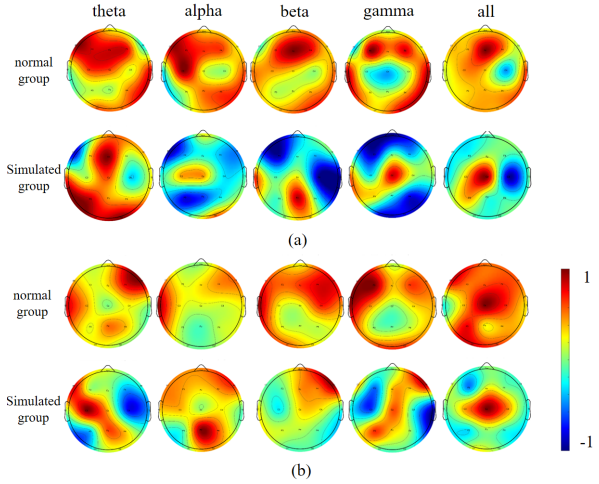


Figure 2: Topological Maps of Inter-subject Similarity Differences; (a) present results for the Visuospatial Memory, while (b) show results for the Verbal Memory.

In the RSA of two tasks, namely the old-new picture discrimination task and the quadrant judgment task, the RSA values of the normal group showed a substantial increase in the old-new picture discrimination task (Liu et al., 2023). Meanwhile, the enhancement effect of the quadrant judgment task was most pronounced in the theta band and full-band integration, which are closely associated with memory consolidation and hippocampal-cortical communication (Gattas et al., 2023). These results indicate that normal sleep facilitates the alignment between behavioral performance and EEG patterns (Liu et al., 2025). In contrast, the RSA values of the simulated OSA group exhibited almost no increase in both tasks after sleep; the values even showed a decrease across most electrode regions. This finding suggests that OSA disrupts the representational consistency established during normal sleep.

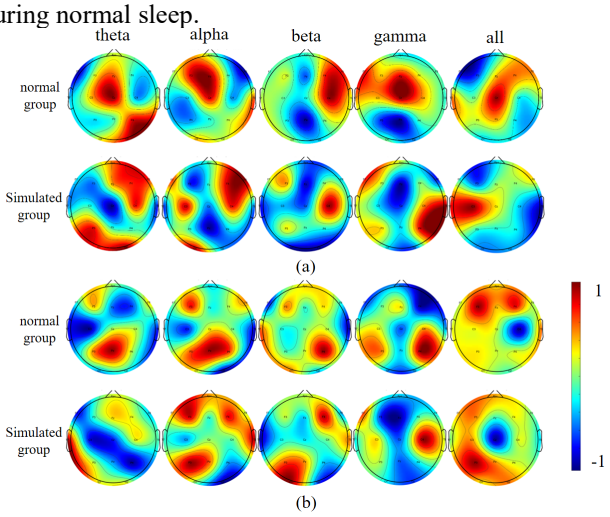


Figure 3: Topological Maps of Representational Similarity

Differences for the Visuospatial Memory; (a) present results of reaction time for old-new picture judgment, while (b) shows results of reaction time for quadrant judgment.

After normal sleep, the representational similarity of reaction time differences in the theta and alpha frequency bands was mainly distributed in the frontocentral and parieto-occipital regions, showing a strong bilateral symmetric pattern (Dai et al., 2017); the beta and gamma frequency bands exhibited more diffuse activation, especially in the central and parietal regions. After full-band integration, the similarity pattern was dominated by the parieto-occipital region. The topographic map of accuracy differences in the normal group showed a similar distribution, Alpha was more prominent in occipital regions, In contrast, the topographic map of the simulated OSA group showed obvious pattern abnormalities. In terms of reaction time differences, the frontocentral activation in the theta and alpha frequency bands was weakened, and the overall similarity intensity was reduced; the beta and gamma frequency bands showed asymmetric distribution, with enhanced activation in the right parietal region and relatively weakened activation in the left (Rajeswari & Jagannath, 2024). In the full frequency band, the overall similarity intensity of the simulated OSA group was significantly lower than that of the normal group, especially in the central and parietal regions. In terms of accuracy differences, the occipital activation in the alpha and beta frequency bands of the simulated OSA group was significantly weakened, the gamma frequency band showed scattered low-similarity regions, and a diffuse and reduced-intensity pattern was presented after full-band integration (Sathyanarayana et al., 2025). Under the simulated OSA condition, the neural representational similarity of verbal memory showed changes in topological distribution in multiple frequency bands, especially the weakening of the low-frequency (theta and alpha) frontoparietal network and the asymmetric enhancement of high-frequency (beta and gamma), which may reflect the interference of OSA-related intermittent hypoxia and sleep fragmentation on the memory encoding and retrieval processes (Liu et al., 2021).

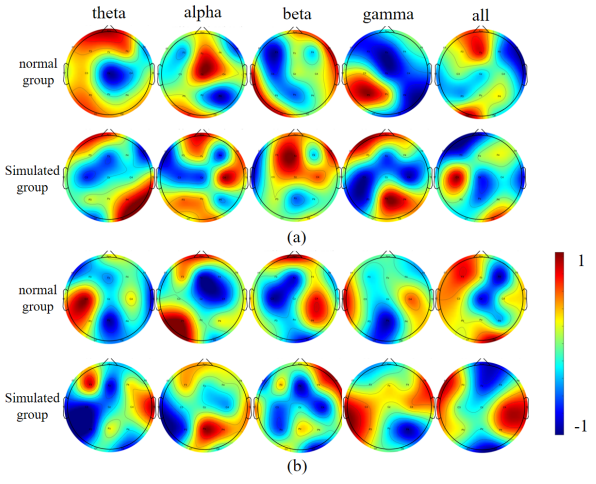


Figure 4: Topological Maps of Representational Similarity Differences for the Verbal Memory; (a) present reaction time results, while (b) show accuracy results.

## Results of Brain Network and PAC Analyses

Following normal sleep, the brain network underlying visuospatial memory underwent positive remodeling in the normal group: the long-range functional connectivity among the frontal, parietal, and occipital regions was substantially strengthened, with consistent results observed in the WPLI and iCOH metrics (Dong et al., 2025;). These findings suggest that normal sleep facilitates the offline consolidation of visuospatial information, as well as the maintenance and retrieval optimization of memory, by enhancing such key long-range connectivity. In contrast, the simulated OSA group exhibited the opposite pattern: the critical long-range functional connectivity of the corresponding brain network was significantly weakened after sleep, accompanied by a marked decline in the network's integrative capacity. This result indicates that normal sleep promotes neural network integration and memory consolidation, while OSA may disrupt this neural network (Xie et al., 2023).

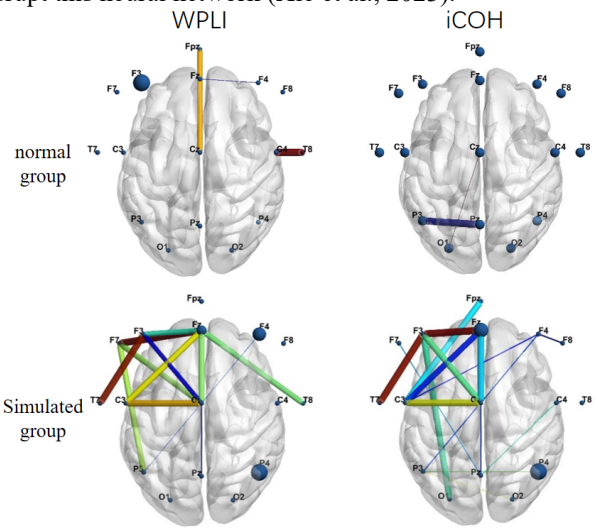


Figure 5: Differential brain network results of the Visuospatial Memory: significant differential edges.

After normal sleep, the brain network subserving verbal memory consolidation underwent beneficial remodeling in the normal group: the long-range functional integration among the frontal, parietal, and occipital regions was markedly enhanced (dominated by red edges), with the strengthened connectivity between the frontal, parietal, and temporal lobes being particularly prominent (Rasch, 2013). The WPLI and iCOH metrics showed a high degree of consistency, suggesting that sleep facilitates the systematic consolidation and cross-regional integration of verbal information (Daneault et al., 2021). In contrast, the simulated OSA group exhibited the opposite pattern: the long-range functional integration of this network was significantly attenuated (dominated by blue edges), with no signs of enhancement.

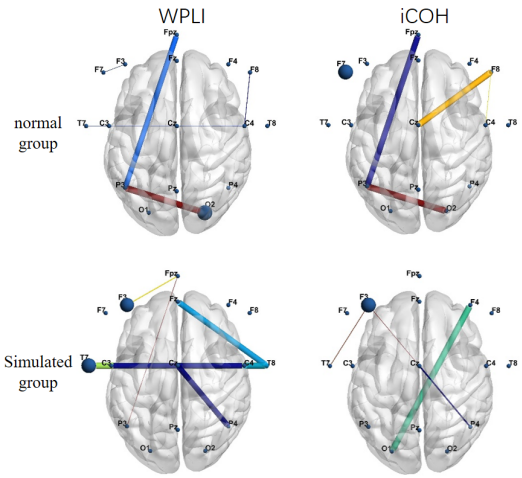


Figure 6: Brain Network Results for the Verbal Memory

In both tasks, the normal group showed a moderate intensity of theta–gamma PAC before sleep, with gamma amplitude mainly modulated around the descending phase to trough of theta (approximately 180°–270° phase window) (Lisman & Jensen, 2013; Lega et al., 2016). The theta-gamma PAC in the normal group was enhanced after sleep, and the MI values increased significantly (all $p < 0.01$) (Klinzing et al., 2019; Bandarabadi et al., 2019). The pre-sleep–post-sleep difference analysis consistently showed that the peak gamma amplitude was more concentrated near the theta trough (approximately 180°–240° optimal phase window), and the MI values in this window were significantly higher than those before sleep. This phase preference is highly consistent with previous studies: the burst of gamma at the theta trough is considered the optimal neural oscillation window for information integration and synaptic plasticity during memory consolidation. In both tasks, the pre-sleep PAC pattern of the simulated group was similar to that of the normal group, and the MI values were at a moderate level. After simulated intervention, there was no systematic significant increase in MI values ($p>0.05$), and the modulation preference of gamma for theta phase remained diffuse, lacking a trend of concentrating toward the theta trough.

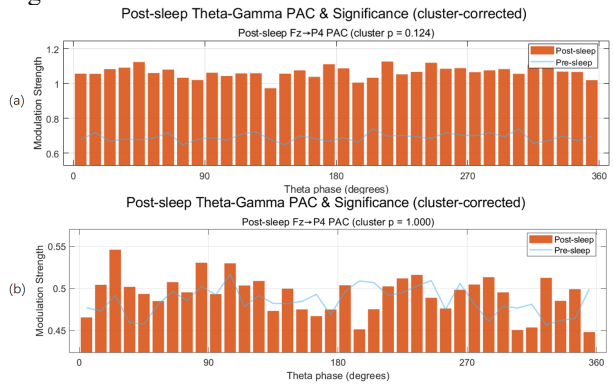


Figure 7: Differential PAC results of the Visuospatial Memory. (a) normal group; (b) simulated OSA group.

This enhancement aligns with the established role of theta-gamma PAC in facilitating hippocampo-neocortical transfer and information integration during systems-level memory consolidation (Rasch & Born, 2013; Klinzing et al., 2019; Lisman & Jensen, 2013). In contrast, simulated OSA prevented these improvements, resulting in unchanged or diffuse PAC patterns and disrupted phase-specific optimization, providing direct neural evidence that sleep fragmentation and intermittent hypoxia impair the offline reorganization of memory consolidation representations.

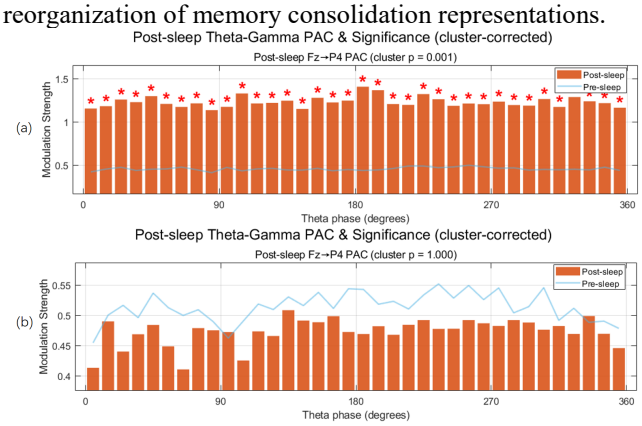


Figure 8: PAC Results for the Verbal Memory.

## Conclusion

This study simulated the intermittent hypoxia and sleep fragmentation characteristic of OSA in healthy volunteers by having them wear masks overnight. Employing a pre-sleep versus post-sleep paired design, we systematically compared the dynamic changes in neural processing underlying visuospatial memory and verbal memory under normal sleep versus simulated OSA conditions. The results demonstrated that normal sleep significantly promoted offline consolidation in both memory tasks, as evidenced by improvements in behavioral performance, enhanced RSA, strengthened long-range brain functional connectivity, and significantly increased theta-gamma PAC strength with optimized phase preference toward the theta trough. These multi-level changes revealed the profound influence of sleep on core cognitive processes such as the representation, maintenance, and consolidation of information in memory consolidation. In contrast, simulated OSA severely disrupted these processes, resulting in the disappearance or even reversal of post-sleep memory consolidation effects: behavioral performance stagnated or deteriorated, inter-individual heterogeneity in neural representations markedly increased, key long-range connectivity weakened, and theta-gamma coupling lacked functional enhancement and phase-specific optimization. These consistent multi-level negative alterations suggest that the combination of sleep fragmentation and intermittent hypoxia may fundamentally impair offline consolidation of memory by interfering with neural oscillatory coordination, and weakening the stability of distributed representations.

## Acknowledgments

This work was supported by the National Natural Science Foundation of China under Grant W2411084; the Chongqing Natural Science Fund Innovation and Development Joint Fund (Municipal Education Commission) project under Grant CSTB2024NSCQ-LZX0121 and the funding of Institute for Advanced Sciences of Chongqing University of Posts and Telecommunications under Grant E011A2022327.

## References

Bandarabadi, M., Gutierrez Herrera, C., Gent, T. C., Bassetti, C., Schindler, K., & Adamantidis, A. R. (2020). A role for spindles in the onset of rapid eye movement sleep. *Nature Communications*, *11*(1), 5247.

Canolty, R. T., Edwards, E., Dalal, S. S., Soltani, M., Nagarajan, S. S., Kirsch, H. E., ... & Knight, R. T. (2006). High gamma power is phase-locked to theta oscillations in human neocortex. *Science*, *313*(5793), 1626–1628.

Chen, G., Taylor, P. A., Qu, X., Molfese, P. J., & Cox, R. W. (2020). Untangling the relatedness among correlations, part III: Inter-subject correlation analysis through Bayesian multilevel modeling for naturalistic scanning. *NeuroImage*, *216*, 116831.

Chen, Y., Zhang, J., Li, X., ... & Wang, Y. (2025). The impact of sleep deprivation on cognitive function in healthy adults: insights from auditory P300 and reaction time analysis. *Frontiers in Neuroscience*, *19*, 1559969.

Dai, Z., de Souza, J., Lim, J., Ho, PM, Chen, Y., Li, J., Thakor, N., & Bezerianos, A. (2017). EEG cortical connectivity analysis of working memory reveals topological reorganization in theta and alpha bands. *Frontiers in Human Neuroscience*, *11*, 237.

Daneault, V., Orban, P., Martin, N., Dansereau, C., Godbout, J., Pouliot, P., Dickinson, P., Gosselin, N., Vandewalle, G., Maquet, P., Lina, J.-M., Doyon, J., Bellec, P., & Carrier, J. (2021). Cerebral functional networks during sleep in young and older individuals. *Scientific Reports*, *11*, 4905.

Daume, J., Kamiński, J., Schjetnan, A. G. P., Salimpour, Y., Khan, U., Kyzar, M., ... & Rutishauser, U. (2024). Control of working memory by phase–amplitude coupling of human hippocampal neurons. *Nature*, *629*(8011), 393-401.

Djonlagic, I. E., Guo, M., Igue, M., Kishore, D., Stickgold, R., & Malhotra, A. (2021). Continuous positive airway pressure restores declarative memory deficit in obstructive sleep apnea. *American Journal of Respiratory and Critical Care Medicine*, *203*(9), 1188–1190.

Dong, M., Wang, Y., Su, C., & Cheng, J. (2025). Distinct EEG spectral and functional connectivity patterns in obstructive sleep apnea patients with excessive daytime sleepiness. *Sleep and Breathing*, *29*(4), 261–272.

Gattas, S., Larson, M. S., Mnatsakanyan, L., Sen-Gupta, I., Vadera, S., Swindlehurst, A. L., Rapp, P. E., Lin, J. J., & Yassa, M. A. (2023). Theta mediated dynamics of human hippocampal-neocortical learning systems in memory formation and retrieval. *Nature Communications*, *14*, 8505.

Giri, B., Kinsky, N., Kaya, U., Maboudi, K., Abel, T., & Diba, K. (2024). Sleep loss diminishes hippocampal reactivation and replay. *Nature*, *630*(8018), 935–942.

Hou, A., Pang, X., Zhang, X., Peng, Y., Li, D., Wang, H., Zhang, Q., Liang, M., & Gao, F. (2022). Widespread aberrant functional connectivity throughout the whole brain in obstructive sleep apnea. *Frontiers in Neuroscience*, *16*, 920765.

Huang, S., Faul, L., & De Brigard, F. (2025). Trial-level representational similarity analysis. *eLife*, reviews preprint.

Hülsemann, M. J., Naumann, E., & Rasch, B. (2019). Quantification of phase-amplitude coupling in neuronal oscillations: Comparison of phase-locking value, mean vector length, modulation index, and generalized-linear-modeling-cross-frequency-coupling. *Frontiers in Neuroscience*, *13*, 573.

Kandeepan, S., Thompson, J. S., & Zendel, B. R. (2023). Inter-subject correlations of EEG reflect subjective arousal and acoustic features of music. *Frontiers in Human Neuroscience*, *17*, 1225377.

Kharas, N., Chelaru, M. I., Eagleman, S., Parajuli, A., & Dragoi, V. (2024). NREM sleep improves behavioral performance by desynchronizing cortical circuits. *Science*, *386*(6724), 892–897.

Kim, J., & Park, M. (2025). Systems memory consolidation during sleep: oscillations, neuromodulators, and synaptic remodeling. *BMB Reports, 58*(10), 425–436.

Klinzing, J. G., Niethard, N., & Born, J. (2019). Mechanisms of systems memory consolidation during sleep. *Nature Neuroscience*, *22*, 1598–1610.

Kriegeskorte, N., Mur, M., & Bandettini, P. A. (2008). Representational similarity analysis – connecting the branches of systems neuroscience. *Frontiers in Systems Neuroscience*, *2*, 4.

Lastra, A. C., Neborak, J. M., & Mokhlesi, B. (2025). Diagnosis and Treatment of Obstructive Sleep Apnea. *JAMA Internal Medicine*, *185*(10), 1465-1474.

Lega, B., Germi, J., & Ranganath, C. (2016). Phase-amplitude coupling supports spatial memory processes. *Current Biology*, *26*(10), R397–R399.

Lisman, J. E., & Jensen, O. (2013). The θ-γ neural code. *Neuron*, *77*(6), 1002–1016.

Liu, J., Xia, T., Chen, D., Yao, Z., Zhu, M., Antony, J. W., Lee, T. M. C., & Hu, X. (2023). Item-specific neural representations during human sleep support long-term memory. *PLoS Biology*, *21*(11), e3002399.

Liu, M., Li, Y., Wang, J., ... & Zhang, L. (2025). Resting-state EEG functional connectivity for brain function analysis and severity classification in obstructive sleep apnea. *IEEE Transactions on Neural Systems and Rehabilitation Engineering*, *33*, 3662–3673.

Liu, S., Shen, J., Li, Y., Wang, J., Wang, J., Xu, J., Wang, Q., & Chen, R. (2021). EEG power spectral analysis of abnormal cortical activations during REM/NREM sleep in obstructive sleep apnea. *Frontiers in Neurology*, *12*, 643855.

Nastase, SA, Gazzola, V., Hasson, U., & Keysers, C. (2019). Measuring shared responses across subjects using intersubject correlation. *Social Cognitive and Affective*

*Neuroscience*, *14* (6), 667–685.
Rajeswari, J., & Jagannath, M. (2024). Brain connectivity analysis based classification of obstructive sleep apnea using electroencephalogram signals. *Scientific Reports*, *14*, 5561.
Rasch, B., & Born, J. (2013). About sleep's role in memory. *Physiological Reviews*, *93*(2), 681-766.
Sathyanarayana, A., Manjunath, S., & Perea, J. A. (2025). Topological data analysis based characteristics of electroencephalogram signals in children with sleep apnea. *Journal of Sleep Research*, *34*(6), e70017.
Simony, E., Honey, C. J., Chen, J., Lositsky, O., Yeshurun, Y., Wiesel, A., & Hasson, U. (2016). Dynamic reconfiguration of the default mode network during narrative comprehension. *Nature Communications*, *7*, 12141.
Suh, S., Kim, H., Dang-Vu, T. T., Joo, E., Shin, C., & Akeju, O. (2021). Effects of obstructive sleep apnea on human spatial navigational memory processing in cognitively normal older individuals. *Journal of Clinical Sleep Medicine*, *17*(5), 943–953.
Tort, A. B. L., Komorowski, R., Eichenbaum, H., & Kopell, N. (2010). Measuring phase-amplitude coupling between neuronal oscillations of different frequencies. *Journal of Neurophysiology*, *104*(2), 1195–1210.
Vinck, M., Oostenveld, R., van Wingerden, M., Battaglia, F., & Pennartz, CMA (2011). An improved index of phase-synchronization for electrophysiological data in the presence of volume-conduction, noise and sample-size bias. *NeuroImage*, *55* (4), 1548–1565.
Wallace, A., & Bucks, R. S. (2013). Memory and obstructive sleep apnea: A meta-analysis. *Sleep*, *36*(2), 203–220.
Wu, K., et al. (2025). Obstructive sleep apnea and structural and functional brain alterations: a brain-wide investigation from clinical association to genetic causality. *BMC Medicine*, *23*(1), 42.
Xie, W., Zeng, L., Huang, L., et al. (2023). Changes in functional connectivity of hippocampal subregions in patients with obstructive sleep apnea after six months of continuous positive airway pressure treatment. *Brain Sciences*, *13*(5), 838.
Zalesky, A., Fornito, A., & Bullmore, E. T. (2010). Network-based statistic: identifying differences in brain networks. *NeuroImage*, *53*(4), 1197–1207.
Zhang, C., Wang, Y., Li, M., ... & Wang, X. (2024). Phase-amplitude coupling in theta and beta bands: A potential electrophysiological marker for obstructive sleep apnea. *Nature and Science of Sleep*, *16*, 1469–1482.
Zhang, X., Xu, H., Yin, S., Gozal, D., & Khalyfa, A. (2025). Obstructive sleep apnea and memory impairments: Clinical characterization, treatment strategies, and mechanisms. *Sleep Medicine Reviews*, *81*, 102092.